JCTC Journal of Chemical Theory and Computation

Article

pubs.acs.org/JCTC

Accurate Reaction Energies in Proteins Obtained by Combining QM/MM and Large QM Calculations

LiHong Hu,[†,‡] Pär Söderhjelm,[†] and Ulf Ryde*[,†]

[†]Department of Theoretical Chemistry, Lund University, Chemical Centre, P.O. Box 124, SE-221 00 Lund, Sweden

[‡]School of Computer Science and Information Technology, Northeast Normal University, Changchun, 130024, People's Republic of China

Supporting Information

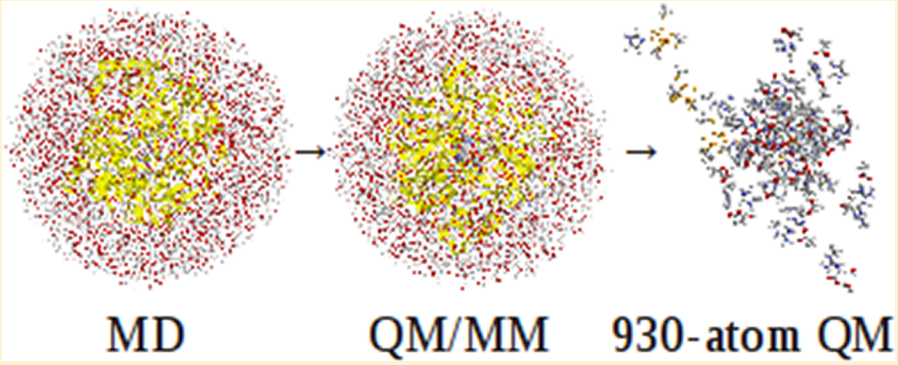

ABSTRACT: We here suggest and test a new method to obtain stable energies in proteins for charge-neutral reactions by running large quantum mechanical (QM) calculations on structures obtained by combined QM and molecular mechanics (QM/MM) geometry optimization on several snapshots from molecular dynamics simulations. As a test case, we use a proton transfer between a metal-bound cysteine residue and a second-sphere histidine residue in the active site of [Ni,Fe] hydrogenase, which has been shown to be very sensitive to the surroundings. We include in the QM calculations all residues within 4.5 Å of the active site, two capped residues on each side of the active-site residues, and all charged groups that are buried inside the protein, which for this enzyme includes three iron−sulfur clusters, in total, 930 atoms. These calculations are performed at the BP86/def2-SV(P) level, but the energies are then extrapolated to the B3LYP/def2-TZVP level with a smaller QM system, and zero-point energy, entropy, and thermal effects are added. We test three approaches to model the remaining atoms of the protein solvent, viz., by standard QM/MM approaches using either mechanical or electrostatic embedding or by using a continuum solvation model for the large QM systems. Quite encouragingly, the three approaches give the same results within 14 kJ/mol, and variations in the size of the QM system do not change the energies by more than 8 kJ/mol, provided that the QM/MM junctions are not moved closer to the QM system. The statistical precision for the average over 10 snapshots is 1−3 kJ/mol.

INTRODUCTION

During the latest decades, quantum-mechanical (QM) calculations have been established as a powerful complement and alternative to experimental methods to study biochemical reactions. In particular, it has repeatedly been shown that they can be used to deduce the reaction mechanisms of enzymes by optimizing intermediates and transition states and comparing activation barriers of alternative reaction pathways.[1−7]

There are two dominant approaches to performing QM calculations on protein reactions. The first is the QM cluster method, in which the active site and neighboring important residues (typically 50−200 atoms) are cut out of the protein and studied in a vacuum or more typically in a continuum solvent with a dielectric constant of ∼4.[1−3] Geometries are normally obtained with basis sets of split-valence quality (keeping one or several atoms fixed around cut bonds), and single-point energies are then calculated on these structures with triple-ζ basis sets. Zero-point energies are obtained from frequency calculations.

The second approach is to treat the active site (still 50−200 atoms) with QM methods and the rest of the enzyme and some surrounding explicit solvent by molecular-mechanics (MM) methods, the QM/MM approach.[5−8] Thus, the method takes a full atomistic account of the surroundings, and it is intended to combine the accuracy of QM calculations with the speed of MM calculations.

The advantage of the QM cluster approach is the small size of the QM system that allows for accurate calculations and a full control of the conformations of the QM system. The disadvantage is that the surroundings are treated only in an approximate implicit manner and that the explicit atoms are

Received: June 18, 2012
Published: October 30, 2012

dx.doi.org/10.1021/ct3005003 | J. Chem. Theory Comput. 2013, 9, 640−649

selected in a subjective and potentially biased way. The advantage of the QM/MM approach is that the entire protein is explicitly included in the calculations. The disadvantage is that the treated system is very large, with an infinite number of possible conformations and many arbitrary choices in the setup. Moreover, there are technical problems in the treatment of chemical bonds between the QM and MM systems (junctions).[6,7,9] In addition, both approaches often ignore effects of entropy and sampling, although there is a growing interest in introducing free-energy methods within the QM/MM paradigm, which also solves the problem of the many possible conformations of the surroundings.[6,7,9−11]

Several groups have studied how QM cluster energies vary with respect to the size of the QM system. For example, we showed that QM cluster energies can differ by over 60 kJ/mol even for QM systems of over 400 atoms, depending on whether atoms have been added to the QM system with respect to their distance to the active site or with respect to group energies from a QM/MM free-energy perturbation technique.[12] Other calculations have indicated differences of 45 kJ/mol between calculations with 300 and 1637 atoms in the QM system.[13] Both of these studies were performed without changing the geometry of the QM systems. Himo et al. have studied the convergence of optimized QM cluster models for several systems and have shown that once the system reaches a certain size (∼200 atoms), the results no longer depend on the dielectric constant of the continuum-solvation model.[14−17]

Moreover, we have shown that QM/MM energies of a 446-atom system (with a fixed geometry) differ from the corresponding QM energy by 7−32 kJ/mol on average, depending on the size of the QM system, as well as the treatment of electrostatic interactions and the junctions.[9] Eriksson and co-workers have shown a variation of QM/MM reaction and activation energies of up to 40 kJ/mol with QM systems of 55−96 atoms (with optimized geometries).[18] Liao and Thiel have observed changes of up to 105 kJ/mol in QM/MM energies when the geometries are optimized with different sizes of the QM system.[19]

In this paper, we suggest and test a new method to obtain stable and accurate energies of reactions inside a protein, based on a combination of MD simulations and QM/MM geometry optimizations, followed by single-point QM cluster calculations, using very big QM systems, employing the information gained in the previous studies. As a test case, we study a simple proton transfer between a metal-bound cysteine (Cys) residue and a second-sphere histidine (His) residue in [Ni,Fe] hydrogenase, which has been shown to be unusually sensitive to the surroundings. This reaction has been employed in several previous studies with different methods,[9,12,20,21] giving an energy of 0 kJ/mol for a minimal QM cluster model but up to 130 kJ/mol with large cluster models.[12]

METHODS

The Protein. The present calculations are based on the 1.81 Å crystal structure of the Ser499Ala mutant [Ni,Fe] hydrogenase from *Desulfovibrio fructosovorans*.[22] The active site is a binuclear Ni−Fe cluster, in which the Fe ion is coordinated to one CO and two CN^- ligands, as well as two Cys residues. These two Cys residues are also ligands of the Ni ion, which is coordinated by two additional Cys residues. Like most other [Ni,Fe] hydrogenases, the enzyme contains three FeS clusters that provide electrons for the reaction. The enzyme also contains an octahedral Mg^{2+} site, which is only 3 Å from the active site.

The setup of the protein was similar to that used in previous calculations.[20,21,23] However, we made a new and more detailed assignment of all protonable residues, based on calculations with PROPKA,[24] H++,[25] a study of the hydrogen-bond pattern around the His residues, the solvent accessibility, and the possible formation of ionic pairs, as is detailed in the Supporting Information. The analysis showed that all potentially charged residues with a solvent accessibility of less than 70% formed direct or water-mediated interactions with other charged residues or metal ions. Therefore, all these residues were assumed to be charged, except Glu-S16 and Glu-25 (an initial S refers to the small subunit, whereas residue numbers without S refer to the large subunit), as is discussed in the Supporting Information, where also the protonation of the His residues are specified. This gave a net charge of +7 for the whole protein.

Once the protonation states of all residues were settled, the protein was protonated and solvated in a truncated octahedron extending at least 8 Å from the protein using the leap module of the Amber software package.[26] The total number of atoms in the simulated system was 50 796.

MD Simulations. MM calculations and MD simulations were performed with the sander module of the Amber software.[4] The protonated and solvated system was optimized by 500 steps of steepest descent minimization, keeping all atoms except solvent water molecules, hydrogen atoms, and active-site atoms restrained to their starting positions with a force constant of 418 kJ/mol/Å^2. The minimization was followed by 20 ps of MD equilibration with a constant pressure and the restraining force reduced to 214 kJ/mol/Å^2. Then, a 200 ps simulation at a constant pressure was performed without any restraints, except for the active-site atoms. Finally, 200 ps of equilibration and 2 ns of production simulation were run with a constant volume and with the active site fixed.

The temperature was kept constant at 300 K, and the pressure was kept constant at 1 atm using the Berendsen weak-coupling algorithm.[27] The nonbonded pair list was updated every 25 steps, and the nonbonded cutoff was 8 Å. Long-range electrostatics were treated using particle-mesh Ewald summation.[28] All bonds involving hydrogen atoms were kept fixed with the SHAKE procedure,[29] allowing for a time step of 2 fs. Snapshots were collected every 200 ps. The MM calculations for the QM/MM optimizations were performed without any periodic boundary conditions or any cutoff for the nonbonded interactions.

QM Calculations. QM calculations were performed on systems of six different sizes, as specified in Table 1. The smallest QM system (F) is a minimal system, consisting of the Fe and Ni ions (both in the low-spin +II state), the CO and the two CN ligands of Fe, the four Cys ligands (Cys-72, 75, 543, and 546; modeled by CH_3S^- groups), and the proton acceptor His-79 (modeled by imidazole). In QM system E, this system was extended with the protonated Glu-25 residue that forms a hydrogen bond to Cys-543. QM system E consists of 46 atoms, and it has a charge of −1. It is shown in Figure 1. We studied the transfer of a proton between Cys-546 and His-79, trying to estimate the relative free energy of the state with the proton on Cys-546 (called the HID state) and the state with the proton on His-79 (called the HIP state), as is shown in Figure 1a and b.

dx.doi.org/10.1021/ct3005003 | J. Chem. Theory Comput. 2013, 9, 640−649

Table 1. Size, Charge, and Description of the Various QM Systems

QM system	# atoms	charge	description
A	930	−2	E capped with two residues on each side, all groups <4.5 Å from F, all metal sites, all buried charged residues
B	845	2	A, except FeS clusters and Lys-225
C	675	1	B, except groups not H-bonded to E
D	651	1	C, but only capped with one residue on each side of F
E	46	−1	F + Glu-25
F	39	−1	Fe, Ni, CO, 2 CN, Cys-72, 75, 543, 546, His-79

In the largest QM system (A), the active site was extended with two capped residues on each side. In addition, all chemical groups within 4.5 Å of the QM system F, as well as all metal sites and all buried charged groups, were included. This gave a total of 930 atoms, and it is shown in Figure 2. We also studied two slightly smaller QM systems, obtained by deleting the three FeS clusters (B) and all charged groups that are not connected to QM system E (C). Finally, we tried to reduce the capping of the active site to one residue (D). Details of the various QM systems are given in the Supporting Information.

QM optimizations, frequency calculations, and QM/MM optimizations with the QM systems E and F as well as single-point energy calculations with the large QM systems A−D were performed with the Becke 1988−Perdew 1986 (BP86) density functional[30,31] together with the def2-SV(P) basis set.[32] The calculations were sped up by expanding the Coulomb interactions in auxiliary basis sets, the resolution-of-identity approximation using the auxiliary basis sets corresponding to the def2-SV(P) basis set.[33,34] The calculations of the big QM systems A−D used also the multipole-accelerated resolution-of-identity *J* approach (marij keyword). The largest calculations involved 3999 electrons and 7558 basis functions. Single-point energy calculations were also performed for QM system E with the three-parameter hybrid B3LYP method, as implemented in the Turbomole package,[35,36] using the def2-TZVP basis set.[5] All QM calculations were run with the Turbomole 6.1 software.[37]

Zero-point energies and thermal corrections to the entropy and Gibbs free energy (at 298 K and 1 atm pressure) were calculated from harmonic frequencies using an ideal-gas rigid-rotor harmonic-oscillator approximation.[38] The frequency calculations were performed on QM system F, and the frequencies were not scaled. In several cases, solvation effects were estimated by single-point calculations using the continuum conductor-like screening model (COSMO).[39,40] These calculations were performed at the same level of theory as the geometry optimization and with default values for all parameters (implying a water-like probe molecule) and a dielectric constant of 4. For the generation of the cavity, we used the optimized COSMO radii in Turbomole (1.30, 2.00, 1.83, 1.72, and 2.16 Å for H, C, N, O, and S, respectively,[41] and 2.0 Å for the metals[42]).

QM/MM Calculations. The QM/MM calculations were performed with the ComQum software.[43,44] In this approach, the protein and solvent are split into three subsystems: System 1 was QM system E, and it was relaxed by QM methods. System 2 consisted of all residues within 6 Å of any atom in system 1 and was relaxed by a full MM minimization in each step of the QM/MM geometry optimization, unless otherwise stated. Finally, system 3 contained the remaining part of the protein and a number of explicitly modeled surrounding solvent molecules. It was kept fixed at the original coordinates.

In the QM calculations, system 1 was represented by a wave function, whereas all the other atoms were represented by an array of partial point charges, one for each atom, taken from MM libraries. Thereby, the polarization of the QM system by the surroundings is included in a self-consistent manner (electrostatic embedding). When there is a bond between systems 1 and 2 (a junction), the hydrogen link-atom approach was employed: The QM system was capped with hydrogen atoms (H link atoms, HL), the positions of which are linearly related to the corresponding carbon atoms (C link atoms, CL) in the full system.[43,45] All atoms were included in the point-charge model, except those of the CL atoms.[9]

The total QM/MM energy in ComQum was calculated as[43,44]

$$E_{\mathrm{QM/MM}} = E^{\mathrm{HL}}_{\mathrm{QM1+ptch23}} + E^{\mathrm{CL}}_{\mathrm{MM123},q_i=0} - E^{\mathrm{HL}}_{\mathrm{MM1},q_i=0} \quad (1)$$

where $E^{\mathrm{HL}}_{\mathrm{QM1+ptch23}}$ is the QM energy of the QM system truncated by HL atoms and embedded in the set of point

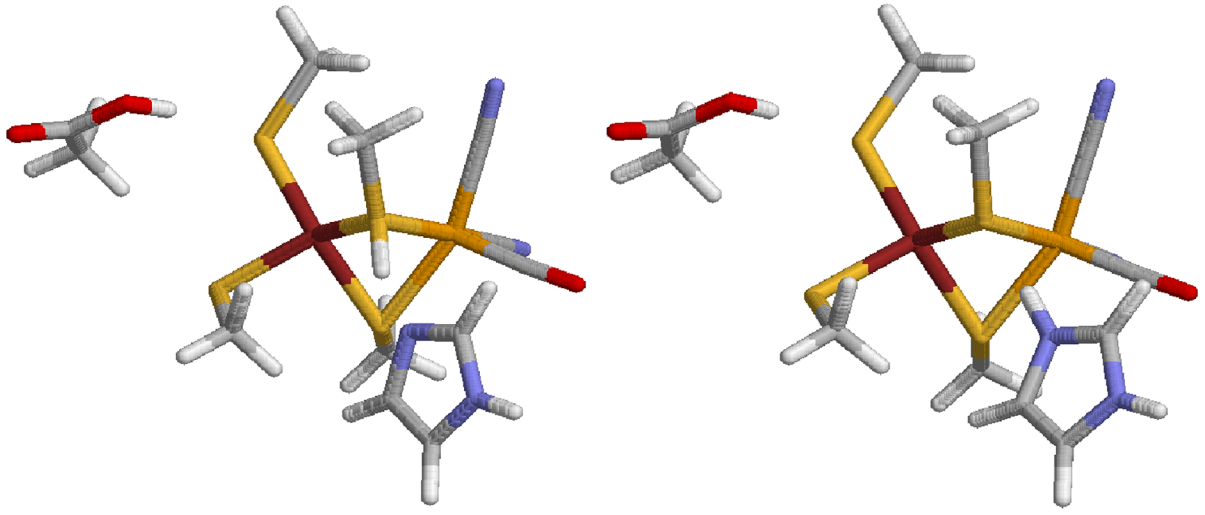

Figure 1. QM system E in the HID (left) and HIP states (right).

dx.doi.org/10.1021/ct3005003 | J. Chem. Theory Comput. 2013, 9, 640−649

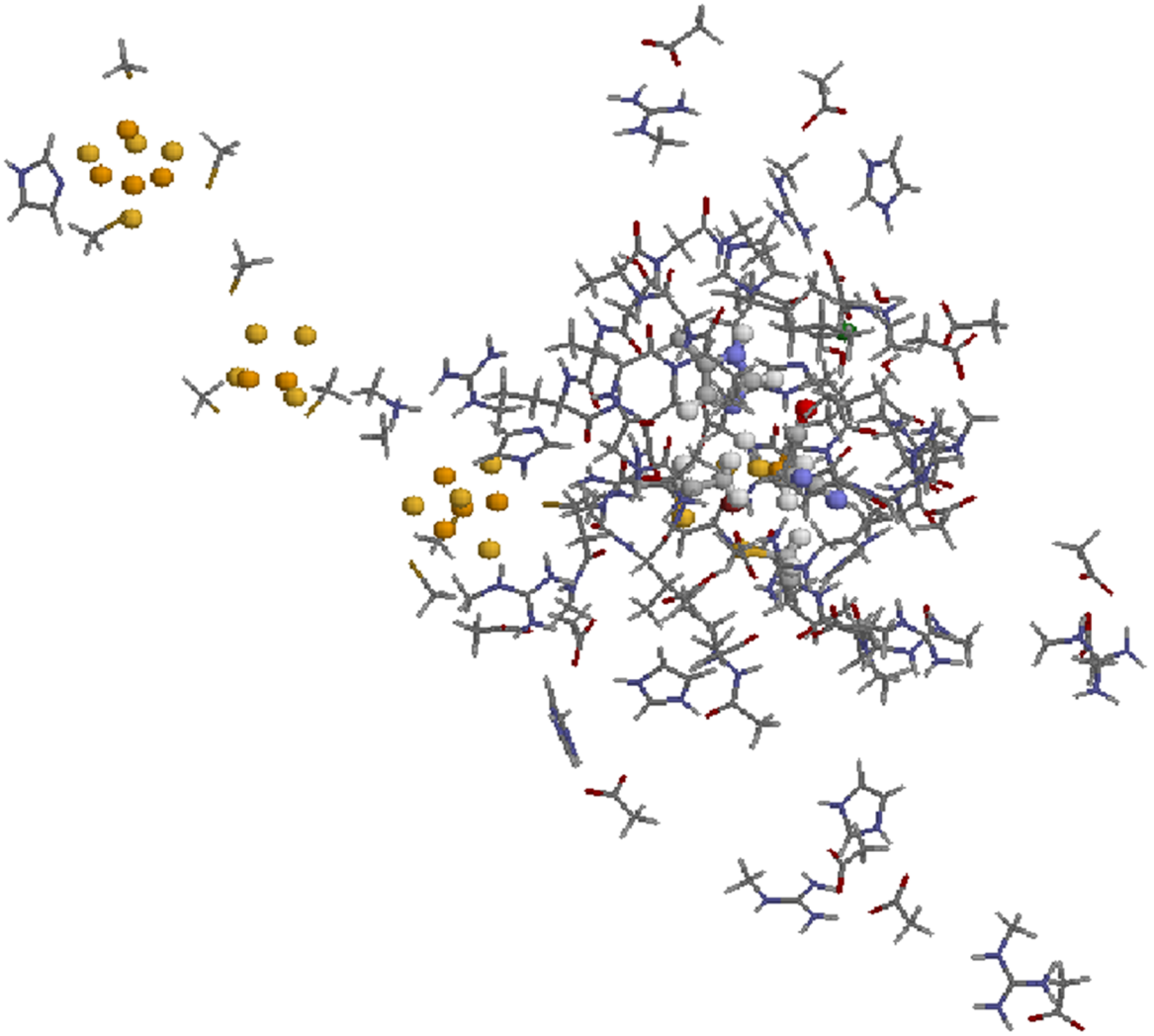

Figure 2. The largest QM system A with 930 atoms. QM system E as well as the metals and sulphide ions are shown in balls-and-sticks representation.

charges modeling systems 2−3 (but excluding the self-energy of the point charges). $E^{HL}_{MM1,q_i=0}$ is the MM energy of the QM system, still truncated by HL atoms, but without any electrostatic interactions. Finally, $E^{CL}_{MM123,q_i=0}$ is the classical energy of all atoms in the system with CL atoms and with the charges of the QM system set to zero (to avoid double-counting of the electrostatic interactions). By this approach, which is similar to the one used in the Oniom method,[46] errors caused by the truncation of the QM system should cancel.

The geometry optimizations were continued until the energy change between two iterations was less than 2.6 J/mol (10^{-6} au) and the maximum norm of the Cartesian gradients was below 10^{-3} au. QM/MM optimizations of both the HID and HIP states were performed for each of the 10 snapshots from the MD simulations. For snapshots 1, 3, 5, 7, and 9 (i.e., those sampled after 0.2, 0.6, 1.0, 1.4, and 1.8 ns), the optimizations were first performed for the HID state with all atoms in system 2 optimized, followed by an optimization of the HIP state with all atoms outside the QM system fixed. For the other five snapshots, the HIP state was first optimized with a relaxed system 2, and the HID state was then optimized with a fixed protein. The HID state was obtained by restraining the S−H distance of the moving proton to 1.405 Å (the distance in optimized structures in a vacuum, where the HID state is a stable minimum).

For the calculations with the large QM systems A−D, we used three different methods to model the surrounding protein. The first was the standard electrostatic-embedding (EE) QM/MM method, described in eq 1; i.e., the QM calculation was performed with a point-charge model of the surroundings, and the MM calculations were performed with zeroed charges for the QM system. The second approach is mechanical embedding (ME) QM/MM. It indicates that the QM calculation is performed without any point-charge model (E^{HL}_{QM1}), and the MM calculations are performed with charges on all atoms, including the QM system (E^{CL}_{MM123}), so that the QM−MM electrostatic interaction energy is calculated at the MM level:

$$E^{ME}_{QM/MM} = E^{HL}_{QM1} + E^{CL}_{MM123} - E^{CL}_{MM1} \quad (2)$$

Finally, we also performed the QM calculation with the COSMO continuum solvent, as a simple way to take into account the surroundings in a continuum manner. We have added to the QM+COSMO energy (with a dielectric constant of 4) also the EE MM correction ($E^{CL}_{MM123,q_i=0} - E^{HL}_{MM1,q_i=0}$), which for these large QM systems with the same positions and

dx.doi.org/10.1021/ct3005003 | J. Chem. Theory Comput. 2013, 9, 640−649

charges of all atoms outside the QM system E consists only of the van der Waals interactions between QM system E and atoms outside the large QM system A−D. This approach will be called COSMO in the following.

We present results obtained from QM/MM optimizations and large QM calculations performed on each of the 10 snapshots from the MD simulations, together with plain averages and the standard error of the mean (i.e., the standard deviation divided by $10^{1/2}$) over these 10 snapshots. Strictly, energies sampled by MD and QM/MM are slightly different, so that the QM and QM/MM energies should be reweighted, but this is normally ignored in QM/MM studies.[5,7]

RESULT AND DISCUSSION

In this paper, we study a proton transfer between Cys-546 and His-79 in *D. fructosovorans* [Ni,Fe] hydrogenase. We try to estimate the relative free energy of the state with the proton on Cys-546 (called the HID state) and the state with the proton on His-79 (called the HIP state). The reaction involves the movement of a proton by ∼0.6 Å, with minimal movements of the other atoms in the active site, as can be seen in Figure 1. Still, the reaction energy is extremely sensitive to the surroundings, giving a reaction energy of 0 kJ/mol for QM system E, but up to 130 kJ/mol in favor of the HIP state for some large QM models.[9]

We here suggest and test a new approach to obtain converged energies for reactions inside proteins, involving a combination of QM, QM/MM, and MD calculations. The method includes the following steps:

- Perform a detailed analysis of the protonation state of all residues as well as of the solvent-accessibility of charged groups
- Run 0.2 + 2 ns MD simulation of the solvated protein
- Select 10 snapshots and perform QM/MM optimizations for the two states
- Calculate BP86/def2-SV(P) energies for a large QM system involving all groups within 4.5 Å of the minimal QM system, all buried charges, and the backbone within two residues of the minimal QM system.
- Calculate single-point B3LYP/def2-TZVP energies on the small QM system.
- Optimize the small QM system freely and calculate the zero-point energy, as well as entropic and thermal corrections for this system.

Details of the calculations are given in the Methods section. Here, results of the various calculations are described.

The results of the analysis of the protonation of the various residues are given in Table S1 in the Supporting Information. It turned out that [Ni,Fe] hydrogenase contains no less than 54 buried charged residues, which all made direct or water-mediated interactions with other charged residues; i.e., they formed ionic pairs or more complicated groups and networks of charges (Figure 2). Therefore, we decided to keep all of them charged, except Glu-S16 and Glu-25, the hydrogen-bond pattern of which showed that they must be protonated and neutral.

It should be noted that this large number of buried charges is a special feature of the hydrogenases, whereas most other proteins have only a few buried charged residues. The reason for this is partly the large number of metal ions in the protein: 15 of the buried charges are ligands of the metal ions, and several of the others are found in the second sphere of the metal ions. Still, many of them are also involved in an intricate network around the active site, which probably tunes the properties of the active site and may be involved in the transport of protons to the active site.

QM/MM Results. Key distances of the 20 QM/MM structures are listed in Table S3 in the Supporting Information. There are only minimal differences between the structures of the HID and HIP states with differences in the active-site metal−ligand bond lengths of 0.01 Å or less. It is only the N−H and S−H distances of the moving proton that change (by 0.60−0.65 Å): In the HID state, the S−H bond length is 1.405 Å (restrained) and the average N−H distance is 1.63 Å, whereas in the HIP state, the average N−H bond length is 1.09 Å and the S−H distance is 2.01 Å.

The QM/MM energies are presented in Table 2. It can be seen that all calculations predict that the HIP state is more stable than the HID state by 36−58 kJ/mol, with an average of 47 ± 2 kJ/mol (all reported uncertainties are standard errors of the mean, i.e., the standard deviation divided by the square root of the number of samples). There is a clear tendency that the five snapshots for which system 2 was optimized for the HID state (S1, S3, S5, S7, and S9) give a smaller energy difference than those optimized for the HIP state, 42 ± 2 kJ/mol compared to 53 ± 2 kJ/mol. The QM/MM energy is dominated by the $E_{QM1+ptch}$ term in eq 1: It gives almost the same results as the total QM/MM energy, 49 ± 2 kJ/mol, whereas the MM energy (the difference of the last two terms in eq 1) contributes only −4 to 0 kJ/mol, −1.3 ± 0.4 kJ/mol on average, favoring the HID state. The reason for this is that MM system 2 was kept fixed for the two states (to avoid the multiple-minima problem), so that this term only contains the difference in the van der Waals interactions between the QM system and the surroundings for the two states. The similarity between the results obtained for snapshots with system 2 optimized for the HID or the HIP state shows that there is no major difference between the two states. We have also performed calculations with the QM/MM-PBSA approach,[21] described in the Supporting Information.

Table 2. QM/MM Energy Differences between the HID and HIP States in kJ/mol[a]

	$E_{QM/MM}$	$E_{QM1+ptch}$	E_{MM}
S1	35.8	37.0	−1.1
S2	46.8	48.8	−2.0
S3	41.3	42.6	−1.3
S4	52.4	52.8	−0.4
S5	40.1	41.6	−1.5
S6	51.1	51.1	−0.1
S7	44.6	48.5	−4.0
S8	58.5	58.9	−0.4
S9	46.6	48.6	−2.0
S10	55.0	55.3	−0.3
Av	**47.2**	**48.5**	**−1.3**
SE	**2.2**	**2.1**	**0.4**

[a]The energy terms are defined in eq 1 except that $E_{MM} = E^{CL}_{MM12,q_i=0} - E^{HL}_{MM1,q_i=0}$. The last two lines contain the average (Av) and standard error (SE; i.e., the standard deviation divided by $10^{1/2}$) over the 10 snapshots.

Large QM Calculations. Next, we cut out the 930-atom QM system A in Figure 2 and performed a single-point energy calculation at the BP86/def2-SV(P) level with three different

dx.doi.org/10.1021/ct3005003 | J. Chem. Theory Comput. 2013, 9, 640−649

Table 3. Results of the Calculations with QM System A[a]

	raw QM results			corrections				corrected results		
	ME	COSMO	EE	B3LYP	DFT-D3	ME	EE	ME	COSMO	EE
S1	46.7	54.4	56.2	1.0	−1.4	0.6	0.0	40.8	47.9	49.7
S2	46.4	48.4	71.5	1.9	−2.3	1.9	−0.6	41.9	41.4	64.6
S3	51.4	55.5	64.6	1.4	−3.1	3.1	−0.6	46.7	47.2	56.3
S4	52.0	63.3	75.0	1.6	−2.0	4.5	−0.5	50.2	56.5	68.1
S5	42.0	56.7	65.1	2.7	−2.5	1.2	−0.1	37.3	50.8	59.1
S6	50.3	61.4	67.8	2.2	−2.9	6.4	−0.1	50.0	54.6	61.0
S7	50.5	51.0	59.8	1.9	−2.9	5.4	−0.6	48.7	43.3	52.1
S8	54.0	63.1	79.5	2.7	−2.9	14.3	−0.5	62.1	56.4	72.7
S9	40.5	56.0	63.7	2.5	−1.5	10.6	−0.2	46.1	50.8	58.5
S10	46.5	63.0	78.2	1.3	−1.6	7.3	−0.3	47.5	56.4	71.6
Av	**48.0**	**57.3**	**68.1**	**1.9**	**−2.3**	**5.5**	**−0.4**	**47.1**	**50.5**	**61.4**
SE	**1.4**	**1.7**	**2.5**	**0.2**	**0.2**	**1.4**	**0.1**	**2.1**	**1.7**	**2.5**

[a]The raw QM calculations are performed either in a vacuum (ME), in a COSMO continuum solvent with a dielectric constant of 4, or with a point-charge model of the surroundings (EE). The corrected results include the B3LYP correction (B3LYP/def2-TZVP calculation on QM system E), the DFT-D3 correction, a correction for zero-point energy, entropy, and thermal effects to the Gibbs free energy at 300 K and 1 atm pressure of −6 kJ/mol for all systems, and an $E^{CL}_{MM123} - E^{CL}_{MM1}$ MM correction, which includes electrostatics (ME) for the vacuum results but only the van der Waals term (EE) for the COSMO and EE results. The last two lines contain the average (Av) and standard error (SE) over the 10 snapshots.

approaches: QM calculations in a vacuum (ME), in COSMO continuum solvation, or with the MM point-charge model of the surroundings (EE). The results of these calculations are collected in Table 3. It can be seen that in all calculations, the HIP state is more stable than the HID state. In the vacuum calculations, the energy difference is 41−54 kJ/mol with an average of 48 ± 1 kJ/mol. With the point-charge model, the difference is 56−79 kJ/mol with an average of 68 ± 2 kJ/mol, i.e., 20 kJ/mol larger. The results obtained with the continuum solvent are intermediate between the other two results, 48−63 kJ/mol with an average of 57 ± 2 kJ/mol. Interestingly, there is only little correlation between the three sets of calculations (r^2 = 0.2). In all calculations, there is a difference between the snapshots for which the surroundings were optimized for the HID state and those optimized for the HIP state of 4−12 kJ/mol, e.g., 62 ± 2 and 74 ± 2 kJ/mol with EE. This shows that the HIP state is further stabilized if the surroundings are optimized for this state.

These energies employ the very large QM system A, but they are calculated with a quite small basis set and a rather inaccurate DFT method. Therefore, we made an extrapolation of the energy of each snapshot by calculating the energy of QM system E with the B3LYP/def2-TZVP method. As can be seen from Table 3, this correction is quite small, 1−3 kJ/mol with an average of 1.9 ± 0.2 kJ/mol in favor of the HIP state. The effect comes mainly from the basis set, somewhat counteracted by the change of functional. Calculations with the even larger def2-QZVPP basis set[37] changed the energies by no more than 1 kJ/mol. This shows that the functional and basis-set effects are quite small. The same correction was obtained also if it was calculated with a point-charge model of the surrounding protein. These results are similar to what has been found before with slightly different basis sets.[20]

Recently, it has been suggested that empirical dispersion corrections are important for reaction energies in proteins calculated with DFT methods, especially for metal sites.[47−50] Therefore, we also estimated the effect of these corrections, using the DFT-D3 method, using single-point energy calculations with the dftd3 program,[51] QM system A, and parameters for the BP86 functional.[52] These corrections are small (owing to the minimal change in geometry) and favor the HID state by 2.3 ± 0.2 kJ/mol (Table 3). Half of the corrections come from the r^{-6} term and the rest from the r^{-8} term.

Next, we estimated also the zero-point energy and thermal corrections for this proton-transfer reaction using frequency calculations of the HID and HIP states. These calculations were performed for the minimal QM system F in a vacuum after optimization, and therefore all 10 snapshots gave the same value, −6 kJ/mol in favor of the HID state. This is slightly smaller than found before (with a different basis set), −9 kJ/mol.[20] Half of the effect comes from the zero-point energies and the rest from entropic and thermal effects.

Finally, we calculated MM corrections to the energies. For the vacuum energies, this was the ME QM/MM correction in eq 2, calculated for QM system A. For these calculations, we need to have charges for the QM system. In accordance with our previous studies,[9] we found that electrostatic-potential (ESP) or Mulliken charges for the whole QM system gave unreliable and unstable results. After some tests, we instead decided to use ESP charges for the central QM system E, but standard Amber charges for the remaining atoms in QM system A (which are the same for the two states, HID and HIP). Then, the average MM correction varied by less than 1 kJ/mol depending on how the ESP charges were calculated (the results in Table 3 use polarized ESP charges, which are different charges for each snapshot and state). This changed the vacuum energies by 1−14 kJ/mol, with an average of 6 ± 1 kJ/mol.

For the QM calculations with a point-charge model, the electrostatic interactions between the QM system and the surroundings are already included in the QM calculations. Therefore, we instead used the EE MM correction ($E^{CL}_{MM123,q_i=0} - E^{HL}_{MM1,q_i=0}$), which is essentially a van der Waals correction. As can be seen from Table 3, this correction is small, −0.4 ± 0.1 kJ/mol on average, because only atoms in the central QM system E change between the two states. The same correction was also added to the COSMO energies.

The final corrected energies are shown in the last three columns in Table 3. It can be seen that the three approaches give energy differences of 47 ± 2 kJ/mol, 50 ± 2 kJ/mol, and 61 ± 2 kJ/mol for ME, COSMO, and EE, respectively. There is

dx.doi.org/10.1021/ct3005003 | J. Chem. Theory Comput. 2013, 9, 640−649

Table 4. Results of the Calculations with QM Systems B, C, and D[a]

QM system	B			C			D		
method	ME	COSMO	EE	ME	COSMO	EE	ME	COSMO	EE
S1	48.0	64.1	56.3	54.9	63.3	54.4	68.6	65.2	64.0
S2	56.7	64.7	72.1	64.0	66.9	68.9	79.3	67.8	81.7
S3	53.6	73.4	63.6	62.6	66.5	63.0	76.1	67.7	74.8
S4	61.7	80.7	78.9	70.0	78.8	74.9	84.0	81.7	86.6
S5	51.8	63.0	62.9	60.3	65.3	59.4	71.7	67.1	70.0
S6	63.3	68.0	74.1	72.9	75.4	71.5	88.2	76.8	83.1
S7	48.3	46.9	63.5	56.6	60.2	60.3	67.5	62.1	73.6
S8	72.0	65.8	82.9	80.7	76.6	79.5	95.9	77.3	93.2
S9	58.1	59.3	66.2	65.7	65.7	63.4	77.4	66.6	72.4
S10	62.0	57.4	78.4	72.6	71.3	74.6	87.3	72.3	88.2
Av	**57.6**	**64.3**	**69.9**	**66.0**	**69.0**	**67.0**	**79.6**	**70.4**	**78.8**
SE	**2.4**	**2.9**	**2.7**	**2.5**	**2.0**	**2.6**	**2.9**	**2.0**	**2.9**

[a]The calculations are performed either with or without a COSMO continuum solvent with a dielectric constant of 4, and either with (EE) or without a point-charge model of the surroundings. All results include corrections for the B3LYP/def2-TZVP method, as well as DFT-D3, zero-point energy, entropy, thermal, and MM corrections. The latter include electrostatics for the ME method but only the van der Waals term for the other two methods. The last two lines of the table contain the average (Av) and standard error (SE) over the 10 snapshots.

still a 6−12 kJ/mol difference between the results obtained for the even and odd-numbered snapshots, but the correlation between the ME and EE results has increased to 0.4.

Analysis of the spin densities in the QM calculations of QM system A showed that we actually have obtained another electronic state in these calculations than in the calculations with the small QM systems E or F: In the latter calculations, we studied the closed-shell state corresponding to low-spin Fe^{II} and Ni^{II}. However, in the large calculations, which necessarily were open-shell calculations owing to the presence of the three FeS clusters, there was almost a unit spin on the Ni ion (0.78−1.07*e*, ∼0.10*e* more in the HIP state than in the HID state, the least in the ME calculations and most in the EE calculations). The active-site Fe ion had only a minor spin of ∼0.2*e*. The distal and medial FeS clusters had close to their expected total spin (18 and 15 unpaired electrons, respectively, indicative of the $Fe^{II}_2Fe^{III}_2$ and Fe^{III}_3 states, respectively, but the proximal FeS cluster had much less spin than expected, ∼16.2 unpaired electrons, compared to 18 unpaired spins expected for the $Fe^{II}_2Fe^{III}_2$ state. The remaining spin was delocalized over the active site (∼0.5*e*) and the surrounding residues (∼0.3*e*). Together, this indicates that the proximal FeS cluster has oxidized the active-site Ni ion to Ni^{III}, attaining the reduced $Fe^{II}_3Fe^{III}$ state itself. Of course, this is an interesting observation, showing that the redox potential of the proximal FeS cluster is higher than that of the Ni−Fe active site in the SI state of [Ni,Fe] hydrogenase from *D. fructosovorans*. All 20 QM calculations gave the same state, independent of the location of the proton between Cys-546 and His-79. A similar state was also obtained if only the proximal cluster was included in the QM system.

QM Systems B−D. To compare with our previous calculations,[9,12,20,21] in which we assumed a Ni^{II}−Fe^{II} state of the active site and the oxidized state of all three FeS clusters, it is better if we can enforce the latter state. Therefore, we performed three additional sets of large QM calculations in which we moved the three FeS clusters to the MM system. In the first of these (QM system B), we only moved the three FeS clusters, together with the Lys-225 residue, which is a second-sphere ligand of the medial [3Fe−4S] cluster. The omission of the proximal [4Fe−4S] cluster is somewhat problematic, because one of its ligands, Cys-S17, has atoms within 3 Å of QM system E. We solved this by including this residue in the QM system, but converting the SG atom to a hydrogen atom, giving an Ala residue. This gave a QM system (B) with 845 atoms, which was studied in the closed-shell Ni^{II}−Fe^{II} state. These closed-shell calculations were much cheaper than the open-shell calculations with QM system A, ∼1 CPU week compared to ∼4 weeks, as detailed in the Supporting Information.

The results of the calculations with QM system B are shown in Table 4. We present only the results including the B3LYP, basis-set, DFT-D3 dispersion, zero-point energy, entropy, thermal, and MM corrections. The B3LYP, basis-set, zero-point energy, entropy, and thermal corrections are the same as those for QM system A (2 and −6 kJ/mol on average, respectively). On the other hand, the DFT-D3 and MM corrections depend on the QM system, although the variation is small: The DFT-D3 and van der Waals (EE) MM corrections are the same as for QM system A, −2.3 ± 0.2 and −0.4 ± 0.1 kJ/mol, respectively, whereas the ME correction is 1 kJ/mol larger, 6 ± 1 kJ/mol. It can be seen that the change in the electronic state and the movement of the FeS clusters to the MM system increase the stability of the HIP state by ∼10 kJ/mol. Thus, the HIP state is predicted to be 58 ± 2, 64 ± 3, and 70 ± 3, for the ME, COSMO, and EE calculations, respectively.

Next, we tested whether the size of the QM system could be reduced without affecting the energies. We first tested the effect of moving to the MM system all charged groups that are not directly connected (within 2.5 Å for any atom) to the active site. This involved seven clusters of charged groups: Arg-283−Asp-386−His-798, Arg-345−Glu-554−Asp-559−His-565, Asp−348−Arg-363, His-464−Asp-529, Glu-642−Arg-684, Arg-766−Glu-776, and Glu-792−Arg-795 together with two bridging water molecules. This gave QM system C with 675 atoms.

This changed the corrected energies by 3−8 kJ/mol for the three approaches (Table 4). In fact, the results of the three approaches now agree within 3 kJ/mol. This shows that buried charges not directly connected to the active site have quite restricted effects of the reaction energies, and the effect is quite well described by a point-charge model.

Finally, we tested reducing the QM system further by moving the junctions of the active-site residues one residue closer to the

active site (in QM systems A−C, all residues in the minimal QM system F were capped by two residues on each side, whereas in QM system D, only one residue on each side was used). However, in practice this led to rather small changes in the QM system because the active-site Cys ligands as well as the proton acceptor His are close in sequence (Cys-72, Cys-75, His-79, Cys-543, Cys-546), and many of the connecting residues are within 4.5 Å of QM system F and therefore included in the big QM systems for that reason. Consequently, only 24 atoms could be moved to the MM system even if we divided two residues (Arg-70 and Ile-544) into two parts (backbone and side chain). This gave rather large changes in the energies for the ME (14 kJ/mol) and EE calculations (12 kJ/mol; cf. Table 4). Therefore, we recommend two capping residues on each side of the active-site residues and no division of residues into two parts.

CONCLUSIONS

In this paper, we suggest a new method to obtain stable and reliable energies of reactions in proteins. It employs a combination of MD sampling, QM/MM geometry optimization, and QM calculations with very large QM systems, as well as standard QM extrapolations. It is based on the experience gained in our and other groups how to make the calculated energies stable.[5,7,9,12,20,21,53]

MD simulations were performed to sample the influence of the surroundings on the QM/MM structures and energies. Such an approach has been used for QM/MM calculations by several groups before.[5,7,19] The results show that there are quite large variations in the energies obtained for the various snapshots, up to 34 kJ/mol. Fortunately, averaging brought the statistical uncertainty (standard error of the mean) down to a reasonable 1−3 kJ/mol for the final energies in Tables 3 and 4. The MD simulations were performed with a fixed QM system F, which is necessary to avoid a costly and error-prone parametrization of the metal-containing active site.[54,55]

Accurate structures of the QM site were then obtained by QM/MM optimizations. To avoid the multiple-minima problem, i.e., the risk that the two states reside in different local minima for any parts of the MM system, we kept the surroundings fixed between the two states, optimizing it for the HID state in snapshots with odd numbers and for the HIP state for snapshots with even numbers.

Next, we calculated accurate energies with very large single-point QM calculations. Previous studies have shown that QM/MM calculations are sensitive to the location of the junctions between the MM and QM system.[7,9] Therefore, we moved these at least two capped residues away from the active site (the calculations on QM system D showed that if the junctions are moved closer, the energies change by up to 14 kJ/mol). Moreover, we have shown that neutral residues have a significant effect only when they are within 4.5 Å of the active site (for a charge-neutral reaction).[9] Therefore, all chemical groups with any atom within 4.5 Å of the minimal QM system were included in the calculations. Finally, our previous results indicated that all buried charges in the protein significantly affect the reaction energy.[9,12] Therefore, we made a thorough examination of all buried groups in the protein, decided which of these are expected to be charged, and included them in the calculations. This led to a QM system of 930 atoms, shown in Figure 2. Calculations of this size are possible today even with standard QM codes and computers, although they are quite costly, at least for open-shell systems. Fortunately, the calculations are trivially parallel (a calculation on each protonation state on 10 snapshots). In such large calculations, all important interactions should be included and the QM calculations should provide proper treatment of polarization, short-range electrostatics, charge transfer, and exchange repulsion.

For these energies, we made standard QM extrapolations to a more accurate functional and larger basis sets on the small QM system. We also calculated the zero-point energy, as well as entropic and thermal corrections to the reaction energy from a vacuum frequency calculation with the small QM system. For the present reaction, these corrections were small and partly canceled, but this is not a general result. The energy corrections were highly reproducible over the 10 snapshots.

Finally, we added MM energy corrections from the surrounding protein in a normal QM/MM manner. We tested three different corrections. First, we calculated standard QM/MM mechanical-embedding energies, i.e., QM calculations in a vacuum, with electrostatic interactions between the QM and MM systems treated at the MM level (eq 2). Second, we used electrostatic-embedding QM/MM calculations (eq 1), i.e., QM energies with a point-charge model of the surroundings and only van der Waals terms in the MM correction. Third, we modeled the surroundings using a COSMO continuum solvation model with a dielectric constant of 4. The MM corrections were quite small, −0.4 ± 0.1 kJ/mol for EE and 6 ± 1 kJ/mol for ME and QM system A, but the ME correction increased to 22 ± 2 kJ/mol for the smaller QM system D, reflecting that electrostatic interactions are moved from QM to MM.

Summing up all energies, we obtained an energy difference between the HID and HIP states of 47−60 ± 2 kJ/mol, depending on whether ME, EE, or COSMO calculations were performed. However, an examination of the spin densities showed that the active site had been oxidized to the Ni^{III} state by the proximal [4Fe−4S] cluster.

In order to compare with previous results, we also performed calculations with the three FeS clusters moved to the MM system, fixing the electronic state of the active site to low-spin Ni^{II}. These calculations indicated that the HIP state was 58−70 ± 3 kJ/mol more stable than the HID state. Moving 17 charged groups that were not directly connected to the active site to the MM system changed the energies to 66−69 ± 3 kJ/mol, indicating that such groups are modeled rather well by point-charge or continuum models

These results are quite similar to our previous estimates of this reaction energy. As mentioned earlier, QM system E gave a difference of 0 kJ/mol (in a vacuum, but 57 kJ/mol in a COSMO solvent), whereas QM systems of different sizes, including only groups close to the small QM system, gave energies of up to 130 kJ/mol (both in a vacuum and in a continuum solvent).[12] However, when the important buried charges are included, the energies stabilized around 40−70 and 60−80 kJ/mol in a vacuum and COSMO, respectively,[12] i.e., close to the present results. With the QTCP (QM/MM thermodynamic cycle perturbation) approach, reaction energies of 33−74 kJ/mol were obtained with different sizes of the QM system (the largest values are for the largest QM systems).[20] We strongly believe that the current result is most reliable and close to the best that can be obtained with today's methods.

It is quite satisfactory that the three approaches (ME, EE, and COSMO) gave quite similar results (within 14 kJ/mol). From a theoretical point of view, the EE approach is expected

to be most accurate, because it includes the polarization of the QM system by the MM system. Of course, it would have been more satisfactory if the MM system would also have been polarizable, but since it is quite far from the reacting atoms in the big QM systems, the effect of this polarization can be expected to be limited. Likewise, the junction between the QM and MM systems is moved at least two residues away from the active site, reducing the risk of problems from the hydrogen link-atom approach.[9] The EE calculations are also fastest and therefore recommended for general use.

A problem with the current approach is that the results vary with the state for which the MM system is relaxed in the QM/MM optimizations. It introduces an uncertainty of 6−16 kJ/mol in the final results. Test calculations (described in the Supporting Information) showed that for this test system, the problem can be solved by optimizing the surroundings for both states, although this may introduce problems with differing local minima for more complicated reactions. Preferably, it should be solved by calculating QM/MM free energies,[10] e.g., by the QTCP approach,[11] as has been done before.[20]

Another problem is the risk of using large QM calculations on QM/MM optimized structures. Liao and Thiel have recently presented results indicating that QM/MM reaction energies change by up to 100 kJ/mol when the optimized QM system is enlarged. However, we believe that these energy differences arise more from the multiple-minima problem than from changes in the QM system, although more investigations are needed before this can be settled. Test calculations show that for the present system, the final reaction free energies change by only 0−8 kJ/mol if a larger QM system (192 atoms) is optimized in the QM/MM calculations (described in the Supporting Information).

In conclusion, our results indicate that the EE results with QM systems A−C have an accuracy of ∼10 kJ/mol, unless the DFT methods have unexpectedly large errors for this type of proton-transfer reaction. In principle, such a conclusion is restricted to the present test case. However, the method is directly applicable to any other protein and reaction that conserves the charge (if the charge changes in the reaction, the energy will depend on neutral residues up to ∼10 Å distance and the bulk solvation energy will become much larger[53]). As mentioned above, for most proteins, the number of buried charges is much smaller, making the size of the QM system smaller. In our experience, the effect of the surrounding enzyme is also smaller for most other proteins, except when proton-transfer reactions are studied.[56] Therefore, we expect that our error estimate is transferable also to other proteins.

■ ASSOCIATED CONTENT

Supporting Information

Setup and protonation of the protein; definition of the QM systems; QM/MM-PBSA methods and results; description of the QM/MM geometries; time-consumption of the calculations; calculations with MM system 2 relaxed for both states; results after geometry optimizations with a larger QM system. This information is available free of charge via the Internet at http://pubs.acs.org/.

■ AUTHOR INFORMATION

Corresponding Author

*E-mail: Ulf.Ryde@teokem.lu.se. Tel.: +46-46 2224502. Fax: +46-46 2228648.

Notes

The authors declare no competing financial interest.

■ ACKNOWLEDGMENTS

This investigation has been supported by grants from the Swedish research council (project 2010-5025), from the Crafoord foundation, and from the Wenner-Gren foundation. It has also been supported by computer resources of Lunarc at Lund University.

■ REFERENCES

(1) Siegbahn, P. E. M.; Borowski, T. *Acc. Chem. Res.* **2006**, *39*, 729−738.
(2) Himo, F. *Theor. Chim. Acta* **2006**, *116*, 232−240.
(3) Siegbahn, P. E. M.; Himo, F. *J. Biol. Inorg. Chem.* **2009**, *14*, 643−651.
(4) Ramos, M. J.; Fernades, P. A. *Acc. Chem. Res.* **2008**, *41*, 689−698.
(5) Lonsdale, R.; Ranaghan, K. E.; Mulholland, A. J. *Chem. Commun.* **2010**, *46*, 2354−2372.
(6) Lin, H.; Truhlar, D. G. *Theor. Chem. Acc.* **2007**, *117*, 185−199.
(7) Senn, H. M.; Thiel, W. *Angew. Chem., Int. Ed.* **2009**, *48*, 1198−1229.
(8) Ryde, U. in *Computational Inorganic and Bioinorganic Chemistry*; Solomon, E. I., King, R. B., Scott, R. A., Eds.; J. Wiley, Sons, Ltd.: Chichester, U.K., 2009; pp 33−42.
(9) Hu, L.; Söderhjelm, P.; Ryde, U. *J. Chem. Theory Comput.* **2011**, *7*, 761−777.
(10) Hu, H.; Yang, W. *Annu. Rev. Phys. Chem.* **2008**, *59*, 573−601.
(11) Rod, T. H.; Ryde, U. *J. Chem. Theory Comput.* **2005**, *1*, 1240−1251.
(12) Hu, L.; Eliasson, J.; Heimdal, J.; Ryde, U. *J. Phys. Chem. A* **2009**, *113*, 11793−11800.
(13) Sumowski, C. V.; Ochsenfeld, C. *J. Phys. Chem. A.* **2009**, *113*, 11734−11741.
(14) Hopmann, K. H.; Himo, F. *J. Chem. Theory Comput.* **2008**, *4*, 1129−1137.
(15) Georgieva, P; Himo, F. *J. Comput. Chem.* **2010**, *31*, 1707−1714.
(16) Sevastik, R.; Himo, F. *Bioorg. Chem.* **2007**, *35*, 444−457.
(17) Liao, R.-Z.; Yu, G.; Himo, F. *J. Chem. Theory Comput.* **2011**, *7*, 1494−1501.
(18) Tian, B.; Strid, Å; Eriksson, L. A. *J. Phys. Chem. B* **2011**, *115*, 1918−1926.
(19) Liao, R.-Z.; Thiel, W. *J. Chem. Theory Comput.* **2012**, *8*, 3793−3803.
(20) Kaukonen, M.; Söderhjelm, P.; Heimdal, J.; Ryde, U. *J. Chem. Theory Comput.* **2008**, *4*, 985−1001.
(21) Kaukonen, M.; Söderhjelm, P.; Heimdal, J.; Ryde, U. *J. Phys. Chem. B* **2008**, *112*, 12537−12548.
(22) Volbeda, A.; Montet, Y.; Vernède, X.; Hatchikian, E. C.; Fontecilla-Camps, J. C. *Int. J. Hydrogen Energy* **2002**, *27*, 1449−1461.
(23) Söderhjelm, P.; Ryde, U. *J. Mol. Struct.: THEOCHEM* **2006**, *770*, 199−219.
(24) Olsson, M. H. M. C.; Søndergaard, R.; Rostkowski, M.; Jensen, J. H. *J. Chem. Theory Comput.* **2011**, *7*, 525−537.
(25) Gordon, J. C.; Myers, J. B.; Folta, T.; Shoja, V.; Heath, L. S.; Onufriev, A. *Nucleic Acids Res.* **2005**, *33*, 368−71.
(26) Case, D. A.; Darden, T. A.; Cheatham, T. E., III; Simmerling, C. L.; Wang, J.; Duke, R. E.; Luo, R.; Crowley, M.; Walker, R. C.; Zhang, W.; Merz, K. M.; Wang, B.; Hayik, S.; Roitberg, A.; Seabra, G.; Kolossvary, I.; Wong, K. F.; Paesani, F.; Vanicek, J.; Wu, X.; Brozell, S. R.; Steinbrecher, T.; Gohlke, H.; Yang, L.; Tan, C.; Mongan, J.; Hornak, V.; Cui, G.; Mathews, D. H.; Seetin, M. G.; Sagui, C.; Babin, V.; Kollman, P. A. *Amber 10*; University of California: San Francisco, 2008.
(27) Berendsen, H. J. C.; Postma, J. P. M.; Van Gunsteren, W. F.; Dinola, A.; Haak, J. R. *J. Chem. Phys.* **1984**, *81*, 3684−3690.
(28) Darden, T.; York, D; Pedersen, L *J. Chem. Phys.* **1993**, *98*, 10089−10092.

(29) Ryckaert, J. P.; Ciccotti, G.; Berendsen, H. J. C. *J. Comput. Phys.* **1977**, *23*, 327−341.
(30) Becke, A. D. *Phys. Rev. A* **1988**, *38*, 3098−3100.
(31) Perdew, J. P. *Phys. Rev. B* **1986**, *33*, 8822−8824.
(32) Weigend, F.; Ahlrichs, R. *Phys. Chem. Chem. Phys.* **2005**, *7*, 3297−3305.
(33) Eichkorn, K.; Treutler, O.; Öhm, H.; Häser, M.; Ahlrichs, R. *Chem. Phys. Lett.* **1995**, *240*, 283−290.
(34) Eichkorn, K.; Weigend, F.; Treutler, O.; Ahlrichs, R. *Theor. Chem. Acc.* **1997**, *97*, 119−126.
(35) Becke, A. D. *J. Chem. Phys.* **1993**, *98*, 1372−1377.
(36) Hertwig, R. H.; Koch, W. *Chem. Phys. Lett.* **1997**, *268*, 345−351.
(37) Treutler, O.; Ahlrichs, R. *J. Chem. Phys.* **1995**, *102*, 346−354.
(38) Jensen, F. *Introduction to Computational Chemistry*; John Wiley & Sons: New York, 1993; pp 298−308.
(39) Klamt, A.; Schüürmann, J. *J. Chem. Soc., Perkin Trans. 2* **1993**, *5*, 799−805.
(40) Schäfer, A.; Klamt, A.; Sattel, D.; Lohrenz, J. C. W.; Eckert, F. *Phys. Chem. Chem. Phys.* **2000**, *2*, 2187−2193.
(41) Klamt, A.; Jonas, V.; Bürger, T.; Lohrenz, J. C. W. *J. Phys. Chem.* **1998**, *102*, 5074−5085.
(42) Sigfridsson, E.; Ryde, U. *J. Comput. Chem.* **1998**, *19*, 377−395.
(43) Ryde, U. *J. Comput.-Aided Mol. Des.* **1996**, *10*, 153−164.
(44) Ryde, U.; Olsson, M. H. M. *Int. J. Quantum Chem.* **2001**, *81*, 335−347.
(45) Reuter, N. I.; Dejaegere, A.; Maigret, B.; Karplus, M. *J. Phys. Chem.* **2000**, *104*, 1720−1735.
(46) Svensson, M.; Humbel, S.; Froese, R. D. J.; Matsubara, T.; Sieber, S.; Morokuma, K. *J. Phys. Chem.* **1996**, *100*, 19357−19363.
(47) Goerigk, L.; Grimme, S. *Phys. Chem. Chem. Phys.* **2011**, *13*, 6670−6688.
(48) Siegbahn, P. E. M.; Blomberg, M. R. A.; Chen, S.-L. *J. Chem. Theory Comput.* **2010**, *6*, 2040−2044.
(49) Chen, S.-L.; Blomberg, M. R. A.; Siegbahn, P. E. M. *J. Phys. Chem. B* **2011**, *115*, 4066−4077.
(50) Ryde, U.; Mata, R. A.; Grimme, S. *Dalton Trans.* **2011**, *40*, 11176−11183.
(51) dftd3 software. http://toc.uni-muenster.de/DFTD3/getd3.html (accessed November 2012).
(52) Grimme, S.; Antony, J.; Ehrlich, S.; Krieg, H. *J. Chem. Phys.* **2010**, *132*, 154104.
(53) Genheden, S.; Ryde, U. *J. Chem. Theory Comput.* **2012**, *8*, 1449−1458.
(54) Hu, L.; Ryde, U. *J. Chem. Theory Comput.* **2011**, *7*, 2452−2463.
(55) Hu, L.; Farrokhnia, M.; Heimdal, J.; Shleev, S.; Rulíšek, L.; Ryde, U. *J. Phys. Chem. B* **2011**, *115*, 13111−13126.
(56) Heimdal, J.; Rydberg, P.; Ryde, U. *J. Phys. Chem. B* **2008**, *112*, 2501−2510.